REGULAR ARTICLE

Proteomic dataset of mouse aortic smooth muscle cells

Ursula Mayr[1], Manuel Mayr[1], Xiaoke Yin[1], Shajna Begum[2], Edward Tarelli[3], Robin Wait[2] and Qingbo Xu[1]

[1] Department of Cardiac and Vascular Sciences, St George's, University of London, London, UK
[2] Kennedy Institute of Rheumatology Division, Imperial College London, London, UK
[3] Medical Biomics Centre, St George's, University of London, London, UK

In an accompanying study (in this issue, DOI 10.1002/pmic.200402044), we have characterised the proteome of Sca-1$^+$ progenitor cells, which may function as precursors of vascular smooth muscle cells (SMCs). In the present study, we have analysed and mapped protein expression in aortic SMCs of mice, using 2-DE, MALDI-TOF MS and MS/MS. The 2-D system comprised a non-linear immobilised pH 3–10 gradient in the first dimension (separating proteins with p*I* values of pH 3–10), and 12%T SDS-PAGE in the second dimension (separating proteins in the range 15 000–150 000 Da). Of the 2400 spots visualised, a subset of 267 protein spots was analysed, with 235 protein spots being identified corresponding to 154 unique proteins. The data presented here are the first map of aortic SMCs and the most extensive analysis of SMC proteins published so far. This valuable tool should provide a basis for comparative studies of protein expression in vascular smooth muscle of transgenic mice and is available on our website hhttp://www.vascular-proteomics.com.

Received: December 12, 2004
Revised: March 3, 2005
Accepted: March 31, 2005

Keywords:
Artery / Atherosclerosis / Mouse model / Smooth muscle cells

1 Introduction

Cardiovascular diseases, such as heart attacks and stroke, account for over 50% of all deaths in industrialised countries, clearly outnumbering deaths attributed to malignant or infectious diseases [1, 2]. The mouse was first proposed as a model for atherosclerosis in 1987 and has since become the preferred animal model in cardiovascular research [3–5]. Meanwhile, the generation of apolipoprotein E and low-density lipoprotein receptor-deficient mice is considered one of the most critical advancements in the elucidation of factors affecting atherogenesis.

Correspondence: Dr. Manuel Mayr, Department of Cardiac and Vascular Sciences, St George's, University of London, Cranmer Terrace, London SW17 0RE, UK
E-mail: m.mayr@sgul.ac.uk
Fax: +44-208-725-2812

Abbreviations: GAPDH, glyceraldehyde-3-phosphate dehydrogenase; **Sca1**, stem cell antigen 1; **SMC**, smooth muscle cell

The arterial wall is composed of three layers: the intima, the innermost layer lined with endothelial cells on the luminal side; the media, consisting of several layers of smooth muscle cells (SMCs); and the adventitia, which is mainly formed of connective tissue. Normally, arterial SMCs are contractile and not well responsive to growth factors. However, exposure to stress stimuli, *e.g.*, elevated levels of serum cholesterol, hypertension, diabetes mellitus, smoking, infectious agents, and obviously combinations of these or as yet unrecognised factors, causes endothelial injury, an initial event that precipitates the atherosclerotic process [6, 7], leading to a prominent structural reorganisation in SMCs with loss of myofilaments and formation of an extensive ER and a large Golgi complex termed synthetic phenotype [8].

Because SMCs play a major role in atherogenesis [1, 7] and numerous investigators use mouse models as an experimental system for atherosclerosis research [9–14], the proteomic analysis of mouse arterial SMCs has to be considered a scientific priority [15].

2 Materials and methods

2.1 Mice and SMC culture

All procedures were performed according to protocols approved by the Institutional Committee for Use and Care of Laboratory Animals. Vascular SMCs from C57BL mice were cultivated from aortas as described elsewhere [16]. SMCs were cultured in DMEM (25 mM glucose, Gibco) supplemented with 15% foetal calf serum, penicillin (100 U/mL), and streptomycin (100 μg/mL). Cells were incubated at 37°C in a humidified atmosphere of 5% CO_2 and passaged by treatment with 0.05% trypsin/0.02% EDTA solution. The purity of SMCs was routinely confirmed by immunostaining with antibodies against α-actin. Experiments were conducted on SMCs achieving subconfluence at passages 15–25.

2.2 2-DE

SMCs were homogenised in lysis buffer (9.5 M urea, 2% CHAPS, 0.8% pharmalyte, pH 3–10 and 1% DTT) containing a cocktail of protease inhibitors (Complete Mini, Roche) and centrifuged at 13 000 × *g* at 20°C for 10 min. A minor pellet containing insoluble proteins remained after lysis in urea buffer and subsequent centrifugation. The supernatant containing soluble proteins was harvested and protein concentration was determined [17] using a modification of the method described by Bradford [18]. Solubilised samples were divided into aliquots and stored at −80°C. For 2-DE, extracts were loaded on non-linear (NL) IPG 18-cm strips, pH 3–10 (GE Healthcare). For preparative gels a protein load of 400 μg, was applied to each IPG strip using an in-gel rehydration method. Samples were diluted in rehydration solution (8 M urea, 0.5% CHAPS, 0.2% DTT, and 0.2% pharmalyte pH 3–10) and rehydrated overnight in a reswelling tray. Strips were focussed at 0.05 mA/IPG strip for 60 kVh at 20°C. Once IEF was completed, the strips were equilibrated in 6 M urea containing 30% glycerol, 2% SDS and 0.01% bromophenol blue, with addition of 1% DTT for 15 min, followed by the same buffer without DTT, but with the addition of 4.8% iodoacetamide for 15 min. SDS-PAGE was performed using 12%T, 2.6% C separating polyacrylamide gels without a stacking gel, using the Ettan DALT system (GE Healthcare). The second dimension was terminated when the bromophenol dye front had migrated off the lower end of the gels. After electrophoresis, gels were fixed overnight in methanol:acetic acid:water solution (4:1:5). 2-DE protein profiles were visualised by silver staining using the Plus one silver staining kit (GE Healthcare) with slight modifications to ensure compatibility with subsequent MS analysis. For image analysis, silver-stained gels were scanned in transmission scan mode using a calibrated scanner (GS-800, Bio-Rad). Raw 2-DE gels were analysed using the PDQuest software (Bio-Rad).

2.3 MS

Gel pieces containing selected protein spots were treated overnight with modified trypsin (Promega) according to a published protocol [19] modified for use with an Investigator ProGest (Genomic Solutions, Huntington, UK) robotic digestion system. Following enzymatic degradation, mass spectra were recorded using a quadrupole-TOF (Q-TOF) mass spectrometer (Micromass, Manchester, UK) interfaced to a Micromass CapLC capillary chromatograph. Samples were dissolved in 0.1% aqueous formic acid, injected onto a 300 μm × 5 mm Pepmap C18 column (LC Packings, Amsterdam, The Netherlands), and eluted with an ACN/0.1% formic acid gradient. The capillary voltage was set to 3500 V, and data-dependent MS/MS acquisitions were performed on precursors with charge states of 2, 3, or 4 over a survey mass range of 540–1000. The collision gas was argon, and the collision voltage was varied between 18 and 45 V depending on the charge-state and mass of the precursor. Initial protein identifications were made by correlation of uninterpreted tandem mass spectra to entries in Swiss-Prot and TREMBL, using ProteinLynx Global Server (V 1.1, Micromass). Alternatively, digests were separated by capillary LC on a reverse-phase column (BioBasic-18, 100 × 0.18 mm, particle size 5 μm, Thermo Electron Corporation) and applied to a LCQ IT mass spectrometer (LCQ Deca XP Plus, Thermo Finnigan). Spectra were collected from the IT mass analyser using full ion scan mode over the *m/z* range 300–2000. MS/MS scans were performed on each ion using dynamic exclusion. Database search was performed using the TurboSEQUEST software (Thermo Finnigan).

MALDI-MS was performed using an Axima CFR spectrometer (Kratos, Manchester, UK). The instrument was operated in the positive ion reflectron mode. CHCA was applied as matrix. Spectra were internally calibrated using trypsin autolysis products. The resulting peptide masses were searched against databases using the MASCOT program [20]. One missed cleavage per peptide was allowed and carbamidomethylation of cysteine as well as partial oxidation of methionine were assumed.

3 Results

Mouse SMCs were cultivated from the aorta of 10-week-old mice and seeded on petri dishes coated with 0.02% gelatin. Cell identity was routinely confirmed by immunohistochemistry, using antibodies specific to smooth muscle markers, α smooth muscle actin and smooth muscle myosin [21–24]. Protein extracts were harvested in lysis buffer and separated by 2-DE [25] using strips with a pH 3–10 NL IPG [26] and large format 12% SDS gels. 2-DE gels were of high quality in terms of resolution. Multiple gels from different primary cells ($n = 4$) were run to ensure consistency in spot patterns. Using the PDQuest software, on average 2400 spots were visualised on a silver-stained 2-D gel with 400 μg of protein sample (Fig. 1).

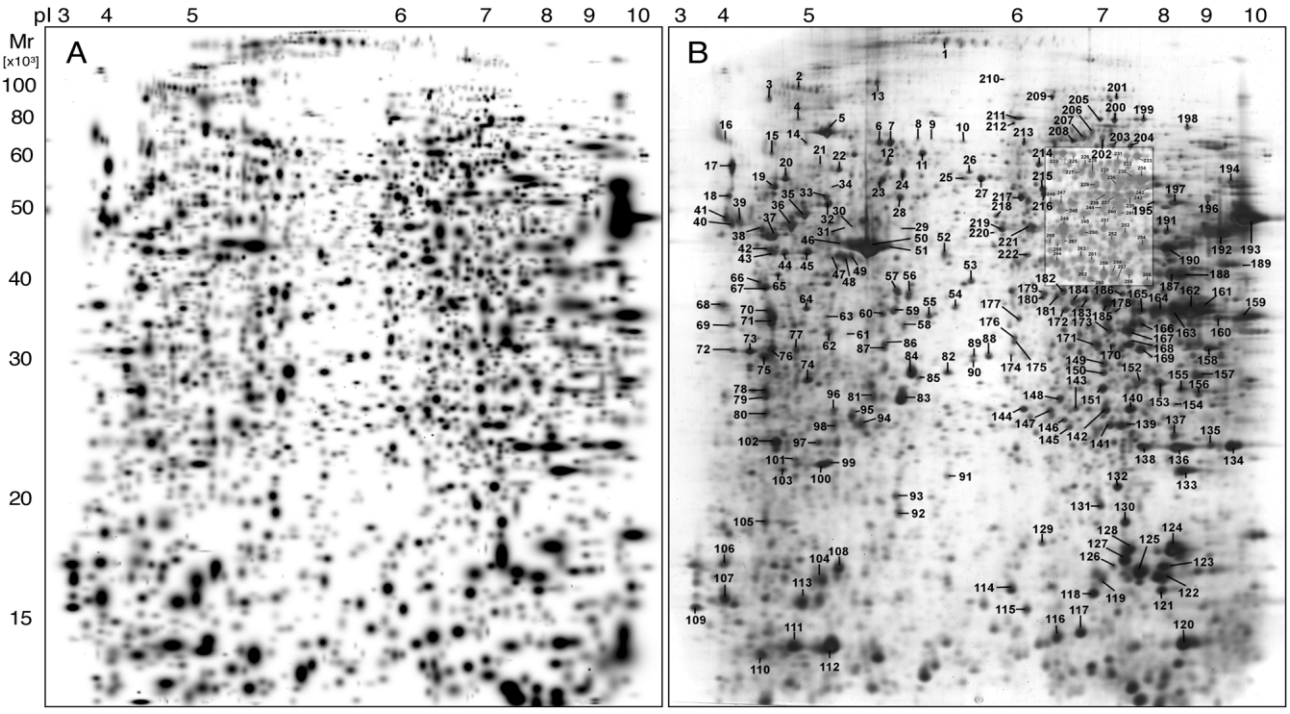

Figure 1. 2-DE map of SMC proteins. SMC protein extract (400 μg) was separated on a pH 3–10NL IPG strip, followed by SDS-PAGE on a 12% gel. Protein spots were visualised by silver staining (Plus One, GE Healthcare). (A) A Gaussian image of the average gel created from four single gels using the PDQuest software (Bio-Rad). On average, 2400 spots were detected in each gel. (B) SMC proteins selected for identification are shown. Selected spots were numbered, excised and subject to in-gel tryptic digestion. Proteins were identified by MS/MS and are listed in Table 1. An enlarged image of the highlighted area is shown in Fig. 2.

From these gels, 267 spots were selected, excised and subject to in gel tryptic digestion [19] using the ProGest robot (Genomic Solutions). Of the picked spots (Figs. 1, 2), 235 positive protein identifications were obtained, representing 154 unique proteins (Table 1). Almost all spots were analysed by MS/MS to ensure accurate identifications. For some spots, additional confirmation was obtained by MALDI MS, and 17 identifications are based on a positive PMF match only.

Several proteins were present as multiple spots on 2-D gels, representing different post-translational modifications that alter the molecular mass and p*I* of the protein. For example, spots 161–164, 166, 167 and 173 were identified as glyceraldehyde 3-phosphate dehydrogenase (GAPDH, theoretical mass/p*I* 35 700 Da/8.45). Of the seven spots, 161–164 form a charge train of molecular masses 37 200 and 37 400 Da with p*I* values of 8.5, 8.3, 8.2 and 7.8, respectively.

Table 1. Protein identification by MS/MS

ID	Protein name	Swiss-Prot entry name	Swiss-Prot accession no.	Calculated MW Da ($\times 10^3$)/p*I*	Observed MW Da ($\times 10^3$)/p*I*	Sequence coverage %	No of peptides
1	Collagen alpha 1(I) chain [Precursor]	CO1A1_MOUSE	P11087	137.9/5.8	142.6/5.7	2.1	2
2	Vascular cell adhesion protein 1 [Precursor]	VCAM1_MOUSE	P29533	81.3/5.2	100.5/4.9	2.0	1
3	Endoplasmin [Precursor]	ENPL_MOUSE	P08113	92.5/4.7	92.5/4.7	7.9	4
4	Heat shock 70-kDa protein 4	HSP74_MOUSE	Q61316	94.1/5.2	77.0/4.9	22.5	4
5	78-kDa glucose-regulated protein [Precursor]	GRP78_MOUSE	P20029	72.4/5.1	72.4/5.1	18.3	8
6	Heat shock cognate 71-kDa protein	HSP7C_MOUSE	P63017	70.9/5.4	70.9/5.3	27.4	13
7	Heat shock cognate 71-kDa protein	HSP7C_MOUSE	P63017	70.9/5.4	70.9/5.4	14.9	7
8	Stress-70 protein, mitochondrial [Precursor]	GRP75_MOUSE	P38647	73.5/5.9	71.5/5.5	14.4	8
9	Stress-70 protein, mitochondrial [Precursor]	GRP75_MOUSE	P38647	73.5/5.9	71.4/5.6	4.0	2
10	Serum albumin [Precursor]	ALBU_BOVIN	P02769	69.3/5.8	71.2/5.8	10.5	5

Table 1. Continued

ID	Protein name	Swiss-Prot entry name	Swiss-Prot accession no.	Calculated MW Da ($\times 10^3$)/p*I*	Observed MW Da ($\times 10^3$)/p*I*	Sequence coverage %	No of peptides
11	Heat-shock related 70-kDa protein 2	HSP72_MOUSE	P17156	69.7/5.6	66.5/5.5	4.7	2
12	Heat shock cognate 71-kDa protein	HSP7C_MOUSE	P63017	70.9/5.4	61.0/5.4	14.9	7
13	GPI-anchored protein p137	GP137_MOUSE	Q60865	73.5/5.2	68.3/5.3	4.6	3
14	Fk509 building protein 9 [Precursor]	FKBP9_MOUSE	Q9Z247	63.0/5.0	70.9/4.9	11.0	121*
15	Ubiquilin-1	UBQL1_MOUSE	Q8R317	62.0/4.9	66.5/4.7	7.9	3
16	Unidentified	–	–	–	71.4/4.2	–	–
17	Calreticulin [Precursor]	CRTC_MOUSE	P14211	48.0/4.3	62.5/4.4	13.7	4
18	Calreticulin [Precursor]	CRTC_MOUSE	P14211	48.0/4.3	52.5/4.4	15.4	3
19	Tumour rejection antigen gp96 [Fragment]	Q8CCY5_MOUSE	Q8CCY5	71.5/4.8	54.6/4.8	3.6	2
20	Vimentin	VIME_MOUSE	P20152	53.6/5.1	56.5/4.8	47.0	187*
21	Unidentified	–	–	–	61.5/5.0	–	–
22	78-kDa glucose-regulated protein [Precursor]	GRP78_MOUSE	P20029	72.4/5.1	60.0/5.1	30.5	17
23	60-kDa heat shock protein, mitochondrial [Precursor]	CH60_MOUSE	P63038	61.0/5.9	56.2/5.3	8.2	3
24	60-kDa heat shock protein, mitochondrial [Precursor]	CH60_MOUSE	P63038	61.0/5.9	58.1/5.4	16.1	7
25	Glucose regulated protein	Q8C2F4_MOUSE	Q8C2F4	56.6/5.8	56.6/5.8	17.6	7
26	T-complex protein 1, epsilon subunit	TCPE_MOUSE	P80316	59.6/5.7	60.0/5.8	18.3	9
27	Protein disulfide isomerase A3 [Precursor]	PDIA3_MOUSE	P27773	56.6/6.0	56.4/5.9	16.0	75*
28	Protein disulfide isomerase A3 [Precursor]	PDIA3_MOUSE	P27773	56.6/6.0	52.1/5.4	2.2	1
29	Ubiquinol-cytochrome-c reductase complex core protein I, mitochondrial [Precursor]	UQCR1_MOUSE	Q9CZ13	52.8/5.8	46.2/5.4	13.5	4
30	Thioredoxin domain containing protein 5 [Precursor]	TXND5_MOUSE	Q91W90	46.4/5.5	47.0/5.2	10.6	3
31	Vimentin	VIME_MOUSE	P20152	53.6/5.1	46.1/5.2	2.2	1
32	ATP synthase beta chain, mitochondrial [Precursor]	ATPB_MOUSE	P56480	56.3/5.2	51.0/5.1	17.2	6
33	Vimentin	VIME_MOUSE	P20152	53.6/5.1	52.3/5.1	14.0	4
34	Vimentin	VIME_MOUSE	P20152	53.6/5.1	54.4/5.1	47.0	187*
35	Vimentin	VIME_MOUSE	P20152	53.6/5.1	48.4/4.9	27.5	9
36	Vimentin	VIME_MOUSE	P20152	53.6/5.1	47.2/4.9	20.7	8
37	Vimentin	VIME_MOUSE	P20152	53.6/5.1	43.7/4.8	12.3	4
38	Vimentin	VIME_MOUSE	P20152	53.6/5.1	46.1/4.6	8.0	2
39	Unidentified	–	–	–	47.7/4.4	–	–
40	Calumenin [Precursor]	CALU_MOUSE	O35887	37.1/4.5	47.4/4.4	4.1	1
41	Calreticulin [Precursor]	CRTC_MOUSE	P14211	48.0/4.3	48.0/4.3	8.9	2
42	Vimentin	VIME_MOUSE	P20152	53.6/5.1	41.4/4.7	11.0	3
43	Vimentin	VIME_MOUSE	P20152	53.6/5.1	41.1/4.7	10.3	3
44	Laminin receptor 1	Q8BNL2_MOUSE	Q8BNL2	32.9/4.8	41.2/4.8	28.1	5
45	Heat shock cognate 71-kDa protein	HSP7C_MOUSE	P63017	70.9/5.4	41.3/4.9	13.2	6
46	Methylosome protein 50	MEP50_MOUSE	Q99J09	36.9/5.1	41.8/5.1	9.4	1
47	Protein disulfide isomerase [Precursor]	PDIA1_MOUSE	P09103	57.1/4.8	41.1/5.1	5.3	2
48	Actin, cytoplasmic 2	ACTG_MOUSE	P63260	41.8/5.3	41.0/5.2	4.2	1
49	Actin, cytoplasmic 2	ACTG_MOUSE	P63260	41.8/5.3	41.0/5.2	4.2	1
50	Actin, cytoplasmic 2	ACTG_MOUSE	P63260	41.8/5.3	41.8/5.3	10.1	4
51	Actin, cytoplasmic 2	ACTG_MOUSE	P63260	41.8/5.3	41.6/5.3	4.3	1
52	Cathepsin D [Precursor]	CATD_MOUSE	P18242	45.0/6.7	41.2/5.7	6.3	1
53	Actin, cytoplasmic 2	ACTG_MOUSE	P63260	41.8/5.3	39.7/5.8	7.5	2
54	Pyruvate kinase, isozyme M2	KPYM_MOUSE	P52480	57.8/7.4	37.3/5.8	28.1	11
55	Pyruvate kinase, M2 isozyme	KPYM_MOUSE	P52480	57.8/7.4	36.5/5.7	6.3	2
56	Unidentified	–	–	–	39.1/5.5	–	–
57	Tubulin alpha-2 chain	TBA2_MOUSE	P05213	50.2/4.9	39.0/5.4	22.4	5
58	Pyruvate dehydrogenase E1 component beta subunit, mitochondrial [Precursor]	ODPB_MOUSE	Q9D051	38.9/6.4	35.8/5.4	13.9	3

Table 1. Continued

ID	Protein name	Swiss-Prot entry name	Swiss-Prot accession no.	Calculated MW Da ($\times 10^3$)/p*I*	Observed MW Da ($\times 10^3$)/p*I*	Sequence coverage %	No of peptides
59	Tubulin, beta 2	Q7TMM9_MOUSE	Q7TMM9	49.9/4.8	37.1/5.4	12.6	4
60	Inorganic pyrophosphatase	IPYR_MOUSE	Q9D819	32.7/5.4	36.5/5.4	42.6	9
61	60S acidic ribosomal protein P0	RLA0_MOUSE	P14869	34.2/5.9	35.5/5.2	17.0	3
62	Transitional endoplasmic reticulum ATPase	TERA_MOUSE	Q01853	89.3/5.1	35.5/5.1	13.8	8
63	60-kDa heat shock protein, mitochondrial [Precursor]	CH60_MOUSE	P63038	61.0/5.9	35.8/5.1	4.5	2
64	Zinc finger protein Aiolos	AIOL_MOUSE	O08900	58.0/5.9	37.4/4.9	19.0	90*
65	Vimentin	VIME_MOUSE	P20152	53.6/5.1	42.1/4.7	20.0	90*
66	Unidentified	–	–	–	39.6/4.6	–	–
67	Tropomyosin beta chain	TPM2_MOUSE	P58774	32.8/4.7	39.4/4.7	27.0	3
68	Nascent polypeptide-associated complex alpha subunit	NACA_MOUSE	Q60817	23.4/4.5	38.1/4.1	19.5	3
69	Unidentified	–	–	–	35.8/4.4	–	–
70	40S ribosomal protein SA	RSSA_MOUSE	P14206	32.6/4.7	37.0/4.7	11.9	2
71	Tropomyosin 1 alpha chain	TPM1_MOUSE	P58771	32.7/4.7	36.0/4.8	43.0	150*
72	Complement component 1, Q subcomponent binding protein, mitochondrial [Precursor]	MA32_MOUSE	O35658	31.0/4.8	34.8/4.4	9.7	3
73	Elongation factor 1-beta	EF1B_MOUSE	O70251	24.6/4.5	34.8/4.5	26.8	3
74	Protein disulfide isomerase [Precursor]	PDIA1_MOUSE	P09103	57.1/4.8	30.4/5.0	6.9	3
75	Tropomyosin alpha 4 chain	TPM4_MOUSE	Q6IRU2	28.3/4.7	33.8/4.7	12.9	2
76	Tropomyosin alpha 3 chain	TPM3_MOUSE	P21107	32.9/4.7	35.1/4.8	7.4	2
77	Actin, cytoplasmic 1	ACTB_MOUSE	P60710	41.7/5.3	34.9/4.9	22.1	8
78	Unidentified	–	–	–	28.8/4.7	–	–
79	Unidentified	–	–	–	27.9/4.7	–	–
80	Tubulin beta-3	TBB3_MOUSE	Q9ERD7	50.4/4.8	25.6/4.7	9.8	3
81	Actin, cytoplasmic 1	ACTB_MOUSE	P60710	41.7/5.3	28.1/5.3	4.3	1
82	Protein disulfide-isomerase A3 [Precursor]	PDIA3_MOUSE	P27773	56.6/6.0	31.4/5.8	18.5	10
83	Actin, cytoplasmic 1	ACTB_MOUSE	P60710	41.7/5.3	27.8/5.4	24.0	107*
84	Actin, cytoplasmic 1	ACTB_MOUSE	P60710	41.7/5.3	31.4/5.5	13.0	73*
85	Prohibitin	PHB_MOUSE	P67778	29.8/5.6	30.7/5.5	26.0	112*
86	Unidentified	–	–	–	35.2/5.4	–	–
87	Unidentified	–	–	–	35.0/5.4	–	–
88	Protein disulfide isomerase associated 3	Q99LF6_MOUSE	Q99LF6	56.7/5.9	33.9/5.9	5.0	2
89	Unidentified	–	–	–	33.9/5.8	–	–
90	Glucose regulated protein	Q8C2F4_MOUSE	Q8C2F4	56.6/5.8	33.3/5.8	10.7	3
91	Vimentin	VIME_MOUSE	P20152	53.6/5.1	21.2/5.7	4.7	2
92	Annexin A1	ANXA1_MOUSE	P10107	38.6/7.2	20.1/5.4	19.1	4
93	Actin, cytoplasmic 1	ACTB_MOUSE	P60710	41.7/5.3	20.6/5.4	4.3	1
94	Actin, cytoplasmic 1	ACTB_MOUSE	P60710	41.7/5.3	24.8/5.3	6.9	2
95	Annexin A1	ANXA1_MOUSE	P10107	38.6/7.2	25.6/5.2	25.7	7
96	Protein disulfide isomerase [Precursor]	PDIA1_MOUSE	P09103	57.1/4.8	26.5/5.1	5.1	2
97	Proteasome subunit beta type 6 [Precursor]	PSB6_MOUSE	Q60692	25.4/5.0	22.7/5.0	16.8	4
98	Glucose regulated protein	Q8C2F4_MOUSE	Q8C2F4	56.6/5.8	24.8/5.1	6.9	2
99	Peroxiredoxin 2	PRDX2_MOUSE	Q61171	21.8/5.2	21.7/5.1	14.1	2
100	Peroxiredoxin 2	PRDX2_MOUSE	Q61171	21.8/5.2	21.6/5.0	58.1	7
101	Unidentified	–	–	–	22.0/4.9	–	–
102	Translationally controlled tumour protein	TCTP_MOUSE	P63028	19.5/4.8	22.7/4.8	28.5	4
103	Prohibitin	PHB_MOUSE	P67778	29.8/5.6	21.6/4.9	11.0	59*
104	Annexin A1	ANXA1_MOUSE	P10107	38.6/7.2	17.0/5.0	8.4	2
105	Myosin regulatory light chain 2, smooth muscle isoform	MLRN_MOUSE	Q9CQ19	19.7/4.8	19.8/4.7	12.3	2
106	Unidentified	–	–	–	18.2/4.2	–	–
107	Lamin A	LAMA_MOUSE	P48678	74.2/6.5	15.6/4.2	15.0	72*
108	Eukaryotic translation initiation factor 5A	IF5A_MOUSE	P63242	16.7/5.1	18.0/5.1	7.8	1

Table 1. Continued

ID	Protein name	Swiss-Prot entry name	Swiss-Prot accession no.	Calculated MW Da ($\times 10^3$)/p*I*	Observed MW Da ($\times 10^3$)/p*I*	Sequence coverage %	No of peptides
109	Calmodulin	CALM_MOUSE	P62204	16.7/4.1	14.7/3.8	36.0	63*
110	Unidentified	–	–	–	12.4/4.6	–	–
111	SH3 domain-binding glutamic acid-rich-like protein	SH3L1_MOUSE	Q9JJU8	12.8/4.9	12.8/4.9	11.4	1
112	Galectin-1	LEG1_MOUSE	P16045	14.7/5.3	12.8/5.1	33.6	4
113	Unidentified	–	–	–	15.9/5.0	–	–
114	Superoxide dismutase [Cu-Zn]	SODC_MOUSE	P08228	15.8/6.0	15.8/6.1	16.3	2
115	Unidentified	–	–	–	14.7/6.1	–	–
116	Histidine triad nucleotide-binding protein 1	HINT1_MOUSE	P70349	13.6/6.4	13.2/6.3	18.4	2
117	40S ribosomal protein S12	RS12_MOUSE	P63323	14.4/7.0	13.5/6.7	18.3	3
118	Nucleoside diphosphate kinase A	NDKA_MOUSE	P15532	17.2/6.8	15.6/6.9	29.6	5
119	Putative RNA-binding protein 3	RBM3_MOUSE	O89086	16.6/6.8	17.0/7.1	37.0	81*
120	Profilin I	PROF1_MOUSE	P62962	14.8/8.5	13.0/8.2	18.7	2
121	Peroxiredoxin 5, mitochondrial [Precursor]	PRDX5_MOUSE	P99029	21.9/9.1	15.7/7.9	23.3	3
122	Peptidyl-prolyl cis-trans isomerase A	PPIA_MOUSE	P17742	17.8/7.9	17.8/7.9	20.2	2
123	Destrin	DEST_MOUSE	Q9R0P5	18.4/8.2	18.1/8.0	24.2	3
124	Cofilin, non-muscle isoform	COF1_MOUSE	P18760	18.4/8.3	18.6/8.2	25.3	3
125	Peptidyl-prolyl cis-trans isomerase A	PPIA_MOUSE	P17742	17.8/7.9	17.9/7.6	20.9	3
126	Unidentified	–	–	–	18.1/7.4	–	–
127	Nucleoside diphosphate kinase B	NDKB_MOUSE	Q01768	17.4/7.0	18.2/7.4	16.5	2
128	Cofilin, muscle isoform	COF2_MOUSE	P45591	18.7/7.7	18.5/7.4	12.1	1
129	Cofilin, non-muscle isoform	COF1_MOUSE	P18760	18.4/8.3	18.7/6.2	12.1	2
130	Transcription factor BTF3	BTF3_MOUSE	Q64152	22.0/9.4	19.8/7.4	9.3	1
131	Peptidyl-prolyl cis-trans isomerase C	PPIC_MOUSE	P30412	22.8/7.0	20.3/7.0	11.8	2
132	Alpha crystallin B chain	CRYAB_MOUSE	P23927	20.1/6.8	20.9/7.3	17.1	3
133	Transgelin 2	TAGL2_MOUSE	Q9WVA4	23.6/6.6	21.4/8.3	31.1	6
134	Transgelin	TAGL_MOUSE	P37804	22.4/8.9	22.3/8.9	14.5	2
135	Transgelin	TAGL_MOUSE	P37804	22.4/8.9	22.4/8.6	21.5	3
136	Peroxiredoxin 1	PRDX1_MOUSE	P35700	22.2/8.3	22.2/8.3	51.8	9
137	Glutathione S-transferase P1	GSTP1_MOUSE	P19157	23.5/8.1	23.4/8.2	9.6	1
138	Superoxide dismutase [Mn], mitochondrial [Precursor]	SODM_MOUSE	P09671	24.6/8.8	22.3/7.6	6.3	1
139	GTP-binding nuclear protein Ran	RAN_MOUSE	P62827	24.4/7.0	24.6/7.3	45.4	11
140	Triosephosphate isomerase	TPIS_MOUSE	P17751	26.6/7.1	26.5/7.5	44.4	8
141	Proteasome subunit alpha type 2	PSA2_MOUSE	P49722	25.8/8.4	24.6/7.2	26.0	126*
142	Triosephosphate isomerase	TPIS_MOUSE	P17751	26.6/7.1	26.3/7.1	55.7	9
143	Protein C14orf166 homolog	CN166 _MOUSE	Q9CQE8	28.3/6.4	26.6/6.6	10.7	2
144	Heat-shock protein beta 1	HSPB1_MOUSE	P14602	23.0/6.1	26.5/6.1	43.1	5
145	Heterogeneous nuclear ribonucleoprotein H1	Q8C2Q7_MOUSE	Q8C2Q7	51.2/6.3	24.4/6.5	12.9	5
146	Triosephosphate isomerase	TPIS_MOUSE	P17751	26.6/7.1	25.2/6.4	22.2	4
147	Peroxiredoxin 6	PRDX6_MOUSE	O08709	24.7/5.7	26.4/6.3	22.0	3
148	Unidentified	–	–	–	27.8/6.3	–	–
149	Annexin A1	ANXA1_MOUSE	P10107	38.6/7.2	32.8/7.1	7.0	1
150	5′-Methylthioadenosine phosphorylase	MTAP_MOUSE	Q9CQ65	31.1/6.7	31.4/7.2	16.0	64*
151	Phosphoglycerate mutase 1	PGAM1_MOUSE	Q9DBJ1	28.7/6.8	29.2/7.1	29.3	5
152	Proteasome subunit alpha type 4	PSA4_MOUSE	Q9R1P0	29.5/7.6	30.2/7.6	65.9	17
153	Heat shock cognate 71-kDa protein	HSP7C_MOUSE	P63017	70.9/5.4	29.9/7.9	10.5	11
154	Glutathione S-transferase Mu 1	GSTM1_MOUSE	P10649	25.8/8.1	27.1/8.2	20.7	4
155	Electron transfer flavoprotein beta-subunit	ETFB_MOUSE	Q9DCW4	27.3/8.6	29.1/8.2	13.1	2
156	Proteasome subunit alpha type 7-like	PSA7L_MOUSE	Q9CWH6	27.9/8.8	28.8/8.4	10.0	2
157	Ras suppressor protein 1	RSU1_MOUSE	Q01730	31.4/8.9	30.8/8.4	34.8	5
158	Voltage-dependent anion-selective channel protein 1	VDAC1_MOUSE	Q60932	32.4/8.6	35.1/8.5	34.1	7
159	Calponin-1	CNN1_MOUSE	Q08091	33.4/9.1	36.2/9.2	6.4	1

Table 1. Continued

ID	Protein name	Swiss-Prot entry name	Swiss-Prot accession no.	Calculated MW Da ($\times 10^3$)/p*I*	Observed MW Da ($\times 10^3$)/p*I*	Sequence coverage %	No of peptides
160	Heterogeneous nuclear ribonucleoproteins A2/B1	ROA2_MOUSE	O88569	36.0/8.7	36.0/8.7	27.0	7
161	Glyceraldehyde 3-phosphate dehydrogenase	G3P_MOUSE	P16858	35.7/8.5	38.0/8.5	15.4	4
162	Glyceraldehyde 3-phosphate dehydrogenase	G3P_MOUSE	P16858	35.7/8.5	37.1/8.3	28.0	6
163	Glyceraldehyde-3-phosphate dehydrogenase	G3P_MOUSE	P16858	35.7/8.5	37.4/8.2	24.4	5
164	Glyceraldehyde 3-phosphate dehydrogenase	G3P_MOUSE	P16858	35.7/8.5	37.2/7.8	18.4	4
165	Annexin A2	ANXA2_MOUSE	P07356	38.5/7.5	37.2/7.6	37.0	8
166	Glyceraldehyde 3-phosphate dehydrogenase	G3P_MOUSE	P16858	35.7/8.5	35.9/7.5	4.2	1
167	Glyceraldehyde 3-phosphate dehydrogenase	G3P_MOUSE	P16858	35.7/8.5	35.6/7.5	31.3	6
168	Voltage-dependent anion-selective channel protein 2	VDAC2_MOUSE	Q60930	31.7/7.4	35.2/7.5	18.3	4
169	Guanine nucleotide-binding protein beta subunit 2-like 1	GBLP_HUMAN	P63244	35.1/7.6	35.1/7.6	44.1	10
170	Electron transfer flavoprotein alpha-subunit, mitochondrial [Precursor]	ETFA_MOUSE	Q99LC5	35.0/8.6	35.2/7.2	21.6	6
171	Esterase D	ESTD_MOUSE	Q9R0P3	34.9/8.5	35.2/7.0	22.8	5
172	PDZ and LIM domain protein 1	PDLI1_MOUSE	O70400	35.7/6.4	37.3/6.4	20.6	5
173	Glyceraldehyde 3-phosphate dehydrogenase	G3P_MOUSE	P16858	35.7/8.5	35.6/7.2	59.2	15
174	Gag protein	Q6YIY0_MOUSE	Q6YIY0	60.3/7.6	34.3/6.0	11.6	4
175	Glucose regulated protein	Q8C2F4_MOUSE	Q8C2F4	56.6/5.8	35.3/6.1	7.9	2
176	Protein disulfide isomerase A3 [Precursor]	PDIA3_MOUSE	P27773	56.6/6.0	35.4/6.1	2.4	1
177	Protein C14orf166 homolog	CN166_MOUSE	Q9CQE8	28.2/6.4	36.5/6.1	8.2	1
178	Annexin A2	ANXA2_MOUSE	P07356	38.5/7.5	37.1/7.2	13.6	3
179	Transaldolose	TALDO_MOUSE	Q93092	37.4/6.6	39.0/6.2	3.3	1
180	Unidentified	–	–	–	38.8/6.2	–	–
181	Glucose regulated protein	Q8C2F4_MOUSE	Q8C2F4	56.6/5.8	38.9/6.3	13.7	4
182	Heat shock cognate 71-kDa protein	HSP7C_MOUSE	P63017	70.9/5.4	39.2/6.4	12.7	6
183	LIM and SH3 domain protein 1	LASP1_MOUSE	Q61792	30.0/6.6	38.8/6.8	5.3	2
184	Annexin A1	ANXA1_MOUSE	P10107	38.6/7.2	38.6/6.5	18.0	4
185	Annexin A1	ANXA1_MOUSE	P10107	38.6/7.2	38.6/7.2	35.7	9
186	Alcohol dehydrogenase [NADP+]	AK1A1_MOUSE	Q9JII6	36.5/6.9	39.0/7.3	7.1	2
187	Fructose-bisphosphate aldolase A	ALDOA_MOUSE	P05064	39.2/8.4	40.1/8.2	19.0	5
188	Fructose-bisphosphate aldolase A	ALDOA_MOUSE	P05064	39.2/8.4	40.0/8.3	27.6	6
189	Aspartate aminotransferase, mitochondrial [Precursor]	AATM_MOUSE	P05202	47.4/9.1	40.6/8.8	12.6	3
190	Phosphoglycerate kinase 1	PGK1_MOUSE	P09411	44.4/7.5	41.5/8.1	12.7	3
191	Fumarate hydratase, mitochondrial [Precursor]	FUMH_MOUSE	P97807	54.4/9.1	45.3/8.1	2.8	3
192	47-kDa heat shock protein [Precursor]	HSP47_MOUSE	P19324	46.6/8.9	45.6/8.7	20.6	6
193	Elongation factor 1-alpha 1	EF1A1_MOUSE	P10126	50.1/9.1	50.1/9.1	21.6	6
194	Unidentified	–	–	–	55.7/8.9	–	–
195	ATP synthase alpha chain, mitochondrial [Precursor]	ATPA_MOUSE	Q03265	59.8/9.2	51.0/7.8	11.2	3
196	Unidentified	–	–	–	52.4/8.5	–	–
197	ATP synthase alpha chain, mitochondrial [Precursor]	ATPA_MOUSE	Q03265	59.8/9.2	51.1/8.2	10.3	3
198	Splicing factor 1	SF01_MOUSE	Q64213	70.4/9.0	74.4/8.3	3.5	2
199	Aconitate hydratase, mitochondrial [Precursor]	ACON_MOUSE	Q99KI0	85.5/8.1	79.1/7.6	3.7	2
200	Far upstream element binding protein 2	FUBP2_RAT	Q99PF5	74.2/6.4	78.9/7.2	9.4	4
201	Unidentified	–	–	–	93.2/7.3	–	–
202	Caldesmon 1	Q8VCQ8_MOUSE	Q8VCQ8	60.5/7.0	71.6/7.1	6.4	3
203	Unidentified	–	–	–	70.0/7.2	–	–
204	Far upstream element binding protein 1	FUBP1_MOUSE	Q91WJ8	68.5/7.7	69.9/7.5	5.5	3
205	Unidentified	–	–	–	79.1/7.0	–	–

Table 1. Continued

ID	Protein name	Swiss-Prot entry name	Swiss-Prot accession no.	Calculated MW Da ($\times 10^3$)/p*I*	Observed MW Da ($\times 10^3$)/p*I*	Sequence coverage %	No of peptides
206	Caldesmon 1	Q8VCQ8_MOUSE	Q8VCQ8	60.5/7.0	72.2/6.9	3.0	1
207	Caldesmon 1	Q8VCQ8_MOUSE	Q8VCQ8	60.5/7.1	71.7/6.7	27.0	124*
208	Filamin A	FLNA_MOUSE	Q8BTM8	281.2/5.7	71.3/6.5	3.7	1
209	Programmed cell death 6 interacting protein	PDC6I_MOUSE	Q9WU78	96.0/6.2	93.4/6.3	13.7	7
210	Vinculin	VINC_MOUSE	Q64727	116.6/5.8	107.4/6.0	3.0	2
211	Fructose-bisphosphate aldolase A	ALDOA_MOUSE	P05064	39.2/8.4	79.8/6.1	8.3	1
212	Moesin	MOES_MOUSE	P26041	67.6/6.2	77.0/6.0	3.3	2
213	Unidentified	–	–	–	71.0/6.1	–	–
214	Dihydropyrimidinase related protein-2	DPYL2_MOUSE	O08553	62.2/6.0	61.8/6.2	10.7	4
215	3-Phosphoglycerate dehydrogenase	Q8C603_MOUSE	Q8C603	56.6/6.3	54.2/6.2	11.5	4
216	Aldehyde dehydrogenase, mitochondrial [Precursor]	ALDH2_MOUSE	P47738	56.5/7.5	51.5/6.2	20.6	6
217	T-complex protein 1, beta subunit	TCPB_MOUSE	P80314	57.3/6.0	52.3/6.1	16.6	6
218	Heat shock cognate 71-kDa protein	HSP7C_MOUSE	P63017	70.9/5.4	48.4/5.9	23.2	12
219	60-kDa heat shock protein, mitochondrial [Precursor]	CH60_MOUSE	P63038	70.0/5.9	46.1/6.0	18.7	7
220	Ornithine aminotransferase, mitochondrial [Precursor]	OAT_MOUSE	P29758	48.4/6.2	45.2/5.9	26.9	9
221	Unidentified	–	–	–	47.1/6.2	–	–
222	Septin 2	SEPT2_MOUSE	P42208	41.5/6.1	41.5/6.1	36.6	9
223	WD-repeat protein 1	WDR1_MOUSE	O88342	66.4/6.1	66.9/6.3	26.7	15
224	WD-repeat protein 1	WDR1_MOUSE	O88342	66.4/6.1	66.9/6.4	10.1	5
225	WD-repeat protein 1	WDR1_MOUSE	O88342	66.4/6.2	66.3/6.5	3.1	1
226	Bifunctional purine biosynthesis protein PURH	PUR9_MOUSE	Q9CWJ9	64.2/6.3	61.8/6.7	71.6	32
227	Stress-induced-phosphoprotein 1	STIP1_MOUSE	Q60864	62.6/6.4	60.0/6.6	25.6	11
228	T-complex protein 1, zeta subunit	TCPZ_MOUSE	P80317	57.9 /6.7	58.6/6.9	8.5	4
229	Dihydrolipoyl dehydrogenase, mitochondrial [Precursor]	DLDH_MOUSE	O08749	54.2/8.0	54.9/6.9	11.2	4
230	T-complex protein 1, zeta subunit	TCPZ_MOUSE	P80317	57.9/6.7	58.6/7.1	39.9	17
231	Heterogeneous nuclear ribonucleoprotein L	HNRPL_MOUSE	Q8R081	60.1/6.7	63.1/7.3	4.1	2
232	Unidentified	–	–	–	65.6/7.4	–	–
233	Transketolase	TKT_MOUSE	P40142	67.6/7.2	65.7/7.6	2.9	2
234	Pyruvate kinase, M2 isozyme	KPYM_MOUSE	P52480	57.8/7.4	56.1/7.6	30.6	9
235	Pyruvate kinase, M2 isozyme	KPYM_MOUSE	P52480	57.8/7.4	56.4/7.5	16.6	6
236	Pyruvate kinase, M2 isozyme	KPYM_MOUSE	P52480	57.8/7.4	54.9/7.3	12.4	5
237	Inosine-5′-monophosphate dehydrogenase 2	IMDH2_MOUSE	P24547	55.8/6.8	52.8/7.3	16.0	5
238	Unidentified	–	–	–	52.8/7.1	–	–
239	Adenylyl cyclase-associated protein 1	CAP1_MOUSE	P40124	51.4/7.3	53.0/7.5	12.3	4
240	Glutamate dehydrogenase, mitochondrial [Precursor]	DHE3_MOUSE	P26443	61.3/8.1	51.0/7.2	17.4	7
241	Unidentified	–	–	–	48.0/7.4	–	–
242	Pyruvate kinase, M2 isozyme	KPYM_MOUSE	P52480	57.8/7.4	54.5/7.7	23.2	10
243	Succinyl-CoA:3-ketoacid-coenzyme A transferase 1, mitochondrial [Precursor]	SCOT_MOUSE	Q9D0K2	56.0/8.7	52.6/7.7	6.9	2
244	Elongation factor 2	EF2_MOUSE	P58252	95.3/6.4	50.0/7.1	31.6	27
245	Septin 11	SEP11_MOUSE	Q8C1B7	49.7/6.2	49.0/6.7	11.4	3
246	Protein disulfide isomerase A3 [Precursor]	PDIA3_MOUSE	P27773	56.6/6.0	50.8/6.3	10.7	4
247	Fascin	FSCN1_MOUSE	Q61553	54.3/6.2	51.0/6.3	5.7	2
248	Aldehyde dehydrogenase, mitochondrial [Precursor]	ALDH2_MOUSE	P47738	56.5/7.5	49.2/6.3	21.0	8
249	Alpha enolase	ENOA_MOUSE	P17182	47.0/6.4	47.0/6.4	40.2	11
250	Proliferation-associated protein 2G4	PA2G4_MOUSE	P50580	43.7/6.4	45.0/6.7	17.8	6
251	Alpha enolase	ENOA_MOUSE	P17182	47.0/6.4	46.4/7.1	11.1	2

Table 1. Continued

ID	Protein name	Swiss-Prot entry name	Swiss-Prot accession no.	Calculated MW Da ($\times 10^3$)/p*I*	Observed MW Da ($\times 10^3$)/p*I*	Sequence coverage %	No of peptides
252	Isocitrate dehydrogenase [NADP] cytoplasmic	IDHC_MOUSE	O88844	46.7/6.5	44.2/7.2	57.5	26
253	26S protease regulatory subunit 8	PRS8_MOUSE	P62196	45.6/7.1	44.3/7.4	11.3	3
254	Phosphoglycerate kinase 1	PGK1_MOUSE	P09411	44.4/7.5	41.6/7.6	13.2	3
255	Pyruvate kinase, M2 isozyme	KPYM_MOUSE	P52480	57.8/7.4	39.6/7.7	6.4	2
256	40-kDa peptidyl-prolyl cis-trans isomerase	PPID_MOUSE	Q9CR16	40.6/7.1	40.2/7.4	18.4	6
257	Unidentified	–	–	–	39.8/7.3	–	–
258	Alcohol dehydrogenase class III	ADHX_MOUSE	P28474	39.5/7.6	40.1/7.2	7.8	1
259	Poly(rC)-binding protein 1	PCBP1_HUMAN	Q15365	37.5/6.7	40.1/7.1	34.6	6
260	T-complex protein 1, beta subunit	TCPB_MOUSE	P80314	57.3/6.0	39.8/6.8	3.7	1
261	Macrophage capping protein	CAPG_MOUSE	P24452	39.2/6.73	40.9/6.8	23.3	7
262	Acyl-CoA dehydrogenase, short-chain specific, mitochondrial [Precursor]	ACADS_MOUSE	Q07417	44.9/9.0	40.4/6.7	2.9	1
263	Heterogeneous nuclear ribonucleoprotein A/B	ROAA_MOUSE	Q99020	30.8/7.7	41.2/6.7	39.7	18
264	Protein disulfide isomerase A6 [Precursor]	PDIA6_MOUSE	Q8BK54	48.7/5.1	40.7/6.3	17.5	6
265	Unidentified	–	–	–	42.4/6.3	–	–
266	Acyl coenzyme A thioester hydrolase, mitochondrial [Precursor]	MTE1_MOUSE	Q9QYR9	49.7/6.9	41.9/6.3	19.4	5
267	Unidentified	–	–	–	44.2/6.4	–	–

* MASCOT score of MALDI-TOF MS spectra.

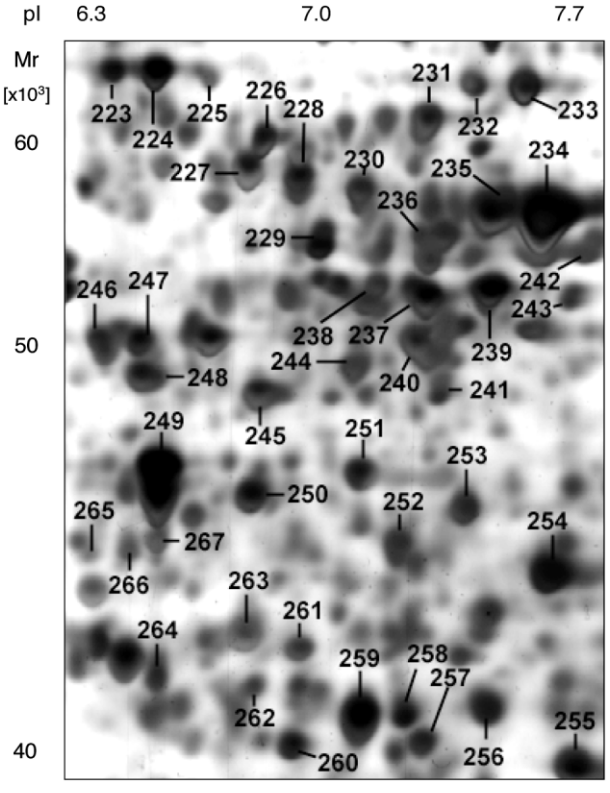

Figure 2. Enlarged area of SMC map, corresponding to the highlighted area in Fig. 1B. Identified proteins are numbered and listed in Table 1.

Here, there is an obvious increase in GAPDH acidity. Phosphorylation of GAPDH has been demonstrated in rabbit muscle [27], porcine brain [28] and a human liver cell line [29]. Phosphorylation would result in a charge shift towards an acidic pH on 2-DE gels providing a possible explanation for the charge heterogeneity observed. However, we were unable to confirm the presence of phosphorylated tryptic peptides by MS/MS sequencing, although this cannot be conclusive, since phosphopeptides frequently go unobserved in digest mixtures unless specific enrichment is undertaken. Notably, modifications other than phosphorylation may also cause a shift towards the acidic direction without affecting M_r. One such is deamidation of asparagine and glutamine residues to aspartic acid and glutamic acid [30]. In spot 162, the doubly charged ion corresponding to the N-terminal tryptic peptide VKVGVNGFGR is observed at m/z 517.31, rather than at the calculated value of 516.80, giving a deconvoluted molecular mass 1 Da greater than expected, which is the mass shift corresponding to deamidation. The MS/MS spectrum of this peptide (Fig. 3A) confirms that there is an aspartic acid residue not asparagine in position 6 (residue mass 115 rather than 114). By contrast, in spot 161, which migrates close to its expected p*I* of 8.45, the corresponding residue is asparagine (Fig. 3B). There was also evidence for partial deamidation of several asparagine residues in spot 164. Thus, at least some of the charge heterogeneity observed in the GAPDH spots can be attributed to deamidation.

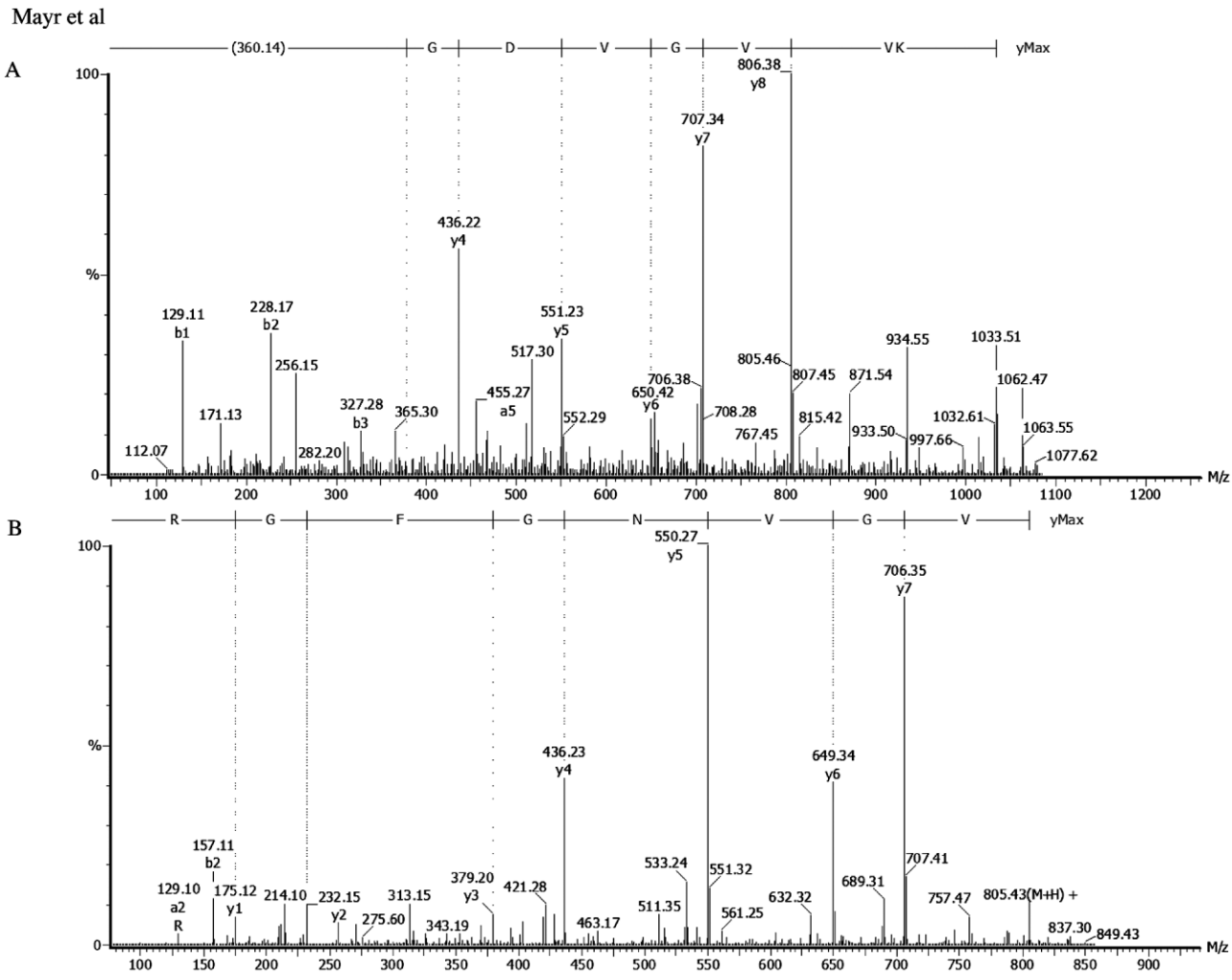

Figure 3. MS/MS spectra. The product ion spectra of the doubly charged tryptic peptides T-(1–10) VKVGVNGFGR at *m/z* 517.31 from spot 162 (A) and T-(3–10) VGVNGFGR at *m/z* 403.22 from spot 161 (B) were both identified as "GAPDH". Note that the MS/MS spectrum from spot 162 shows deamidation of the asparagine in position 6 to aspartic acid giving a deconvoluted molecular mass 1 Da greater than expected, which is the mass shift corresponding to deamidation.

Thirty-two protein spots were not identified. This may have been in part due to an insufficient amount of protein in the spot, despite pooling from replicate gels. Low molecular weight proteins and acidic proteins may also compound this difficulty due to scarcity of tryptic digest sites.

More than half of the identified proteins are either enzymes (34%) or structural proteins (20%), followed by proteins regulating DNA maintenance, transcription and translation (18%), chaperons (11%), antioxidants (5%) and signalling molecules (8%). Notably, fewer proteins involved in cellular signalling and DNA maintenance, transcription, and translation, but more structural proteins were present in arterial SMCs compared to Sca-1$^+$ progenitor cells [31]. Using the "SEARCH SPOT" link on our website, http://www.vascular-proteomics.com, proteins can be listed according to their categories and compared between the different cell lines.

4 Discussion

The current concept of atherosclerosis proposes that SMCs are derived from the media of the artery and migrate to the intima in response to platelet-derived growth factor released by injured endothelial cells and aggregated platelets. However, this concept is challenged by recent findings demonstrating that additional sources of SMCs may contribute to vascular disease [32, 33] and that circulating endothelial progenitor cells can repair denuded endothelium [34].

In an accompanying paper, we characterised the proteome of Sca-1$^+$ progenitor cells, which are derived from embryonic stem cells and may be able to differentiate into vascular SMCs *in vivo* and *in vitro*. In this study, we describe the proteome of differentiated mature SMCs derived from

the mouse aorta. Together these manuscripts provide valuable insights into the protein composition of SMCs and their vascular progenitors.

To date, two protein maps of human SMCs have been published: McGregor *et al.* [35] characterised venous SMCs by dissecting the media from human saphenous veins, while Dupont *et al.* [36] analysed the proteome and secretome of cultured arterial SMCs obtained from human internal mammary arteries. In both maps, proteins were separated by 2-DE and about 120–130 spots were identified. However, unlike the aorta and other large arteries, veins and internal mammary arteries are not very susceptible to spontaneous atherosclerosis. Although several studies have applied proteomic techniques to rat aortic SMCs and have characterised protein changes after growth stimuli [37], during aging [38] and apoptosis [39], no detailed map has been available so far. We have now identified 235 proteins in mouse aortic SMCs, defining the most abundant proteins expressed under cell culture conditions.

Mouse models are an established experimental system for atherosclerosis research and numerous investigators use genetically modified strains to study the molecular mechanisms of vascular pathology including atherogenesis. Previously, we demonstrated that neointima formation was markedly increased in vein grafts of PKCδ-deficient mice compared to wild-type controls. As a first "proof-of-principle" demonstration for combining proteomics and metabolomics, we clarified the underlying mechanism by performing a comparison of SMCs derived from $PKC\delta^{+/+}$ and $PKC\delta^{-/-}$ mice [24]. Similar protein and metabolite changes were found in cardiomyocytes of $PKC\delta^{-/-}$ hearts under *in vivo* conditions [40, 41]. Thus, proteomic and metabolic changes were remarkably consistent in $PKC\delta^{-/-}$ mice, indicating that a single gene mutation is likely to cause alterations of metabolite levels of seemingly unrelated biochemical pathways [42]. To help researchers to understand such systems, a comprehensive and quantitative analysis of proteins and metabolites is required.

The reference map of wild-type SMCs will be a useful tool in the identification and quantification of proteins, which may be differentially expressed, modified or regulated in SMCs of genetically modified mice. It will also be useful in investigating vascular pathology, as proteins derived from vascular SMCs dominate the protein pattern of arterial vessels (Mayr *et al.*, unpublished data). This reference map will be published on our website http://www.vascular-proteomics.com to be accessible for all investigators.

The use of facilities of the Medical Biomics Centre at St. George's, University of London is gratefully acknowledged. This work was supported by grants from the British Heart Foundation and Oak Foundation. Dr. M. Mayr is an intermediate research fellow of the British Heart Foundation.

5 References

[1] Ross, R., *Nature* 1993, *362*, 801–809.

[2] Naghavi, M., Libby, P., Falk, E., Casscells, S. W. *et al.*, *Circulation* 2003, *108*, 1772–1778.

[3] Zhang, S. H., Reddick, R. L., Piedrahita, J. A., Maeda, N., *Science* 1992, *258*, 468–471.

[4] Plump, A. S., Smith, J. D., Hayek, T., Aalto-Setala, K. *et al.*, *Cell* 1992, *71*, 343–353.

[5] Piedrahita, J. A., Zhang, S. H., Hagaman, J. R., Oliver, P. M., Maeda, N., *Proc. Natl. Acad. Sci. USA* 1992, *89*, 4471–4475.

[6] Ross, R., *N. Engl. J. Med.* 1986, *314*, 488–500.

[7] Ross, R., *N. Engl. J. Med.* 1999, *340*, 115–126.

[8] Campbell, J. H., Campbell, G. R., *Curr. Opin. Lipidol.* 1994, *5*, 323–330.

[9] Lindner, V., Fingerle, J., Reidy, M. A., *Circ. Res.* 1993, *73*, 792–796.

[10] Zou, Y., Dietrich, H., Hu, Y., Metzler, B. *et al.*, *Am. J. Pathol* 1998, *153*, 1301–1310.

[11] Lichtman, A. H., Cybulsky, M., Luscinskas, F. W., *Am. J. Pathol* 1996, *149*, 351–357.

[12] O'Neill, T. P., *Toxicol. Pathol* 1997, *25*, 20–21.

[13] Newby, A. C., Baker, A. H., *Curr. Opin. Cardiol.* 1999, *14*, 489–494.

[14] Dietrich, H., Hu, Y., Zou, Y., Dirnhofer, S. *et al.*, *Arterioscler. Thromb. Vasc. Biol.* 2000, *20*, 343–352.

[15] Kanapin, A., Batalov, S., Davis, M. J., Gough, J. *et al.*, *Genome Res.* 2003, *13*, 1335–1344.

[16] Hu, Y., Zou, Y., Dietrich, H., Wick, G., Xu, Q., *Circulation* 1999, *100*, 861–868.

[17] Weekes, J., Wheeler, C. H., Yan, J. X., Weil, J. *et al.*, *Electrophoresis* 1999, *20*, 898–906.

[18] Bradford, M. M., *Anal. Biochem.* 1976, *72*, 248–254.

[19] Shevchenko, A., Wilm, M., Vorm, O., Mann, M., *Anal. Chem.* 1996, *68*, 850–858.

[20] Perkins, D. N., Pappin, D. J., Creasy, D. M., Cottrell, J. S., *Electrophoresis* 1999, *20*, 3551–3567.

[21] Mayr, M., Li, C., Zou, Y., Huemer, U. *et al.*, *FASEB J.* 2000, *14*, 261–270.

[22] Mayr, M., Hu, Y., Hainaut, H., Xu, Q., *FASEB J.* 2002, *16*, 1423–1425.

[23] Mayr, U., Mayr, M., Li, C., Wernig, F. *et al.*, *Circ. Res.* 2002, *90*, 197–204.

[24] Mayr, M., Siow, R., Chung, Y. L., Mayr, U. *et al.*, *Circ. Res.* 2004, *94*, e87–96.

[25] O'Farrell, P. H., *J. Biol. Chem.* 1975, *250*, 4007–4021.

[26] Bjellqvist, B., Ek, K., Righetti, P. G., Gianazza, E. *et al.*, *J. Biochem. Biophys. Methods* 1982, *6*, 317–339.

[27] Kawamoto, R. M., Caswell, A. H., *Biochemistry* 1986, *25*, 657–661.

[28] Wu, K., Aoki, C., Elste, A., Rogalski-Wilk, A. A., Siekevitz, P., *Proc. Natl. Acad. Sci. USA* 1997, *94*, 13273–13278.

[29] Duclos-Vallee, J. C., Capel, F., Mabit, H., Petit, M. A., *J. Gen. Virol.* 1998, *79*, 1665–1670.

[30] Sarioglu, H., Lottspeich, F., Walk, T., Jung, G., Eckerskorn, C., *Electrophoresis* 2000, *21*, 2209–2218.

[31] Yin, X., Mayr, M., Xiao, Q., Mayr, U. *et al.*, *Proteomics* 2005, DOI 10.1002/pmic.200402044.

[32] Hu, Y., Mayr, M., Metzler, B., Erdel, M. *et al.*, *Circ. Res.* 2002, *91*, e13–20.

[33] Hu, Y., Zhang, Z., Torsney, E., Afzal, A. R. *et al.*, *J. Clin. Invest.* 2004, *113*, 1258–1265.

[34] Xu, Q., Zhang, Z., Davison, F., Hu, Y., *Circ. Res.* 2003, *93*, e76–86.

[35] McGregor, E., Kempster, L., Wait, R., Welson, S. Y. *et al.*, *Proteomics* 2001, *1*, 1405–1414.

[36] Dupont, A., Corseaux, D., Dekeyzer, O., Drobecq, H. *et al.*, *Proteomics* 2005, *5*, 585–596.

[37] Patton, W. F., Erdjument-Bromage, H., Marks, A. R., Tempst, P., Taubman, M. B., *J. Biol. Chem.* 1995, *270,* 21404–21410.

[38] Cremona, O., Muda, M., Appel, R. D., Frutiger, S. *et al.*, *Exp. Cell. Res.* 1995, *217*, 280–287.

[39] Taurin, S., Seyrantepe, V., Orlov, S. N., Tremblay, T. L. *et al.*, *Circ. Res.* 2002, *91,* 915–922.

[40] Mayr, M., Metzler, B., Chung, Y. L., McGregor, E. *et al.*, *Am. J. Physiol. Heart Circ. Physiol.* 2004, *287,* H946–H956.

[41] Mayr, M., Chung, Y. L., Mayr, U., McGregor, E. *et al.*, *Am. J. Physiol. Heart Circ. Physiol.* 2004, *287*, H937–H945.

[42] Mayr, M., Mayr, U., Chung, Y. L., Yin, X. *et al.*, *Proteomics* 2004, *4*, 3751–3761.

